N75 27197

FREQUENCY STANDARDS REQUIREMENTS OF THE NASA DEEP SPACE NETWORK TO SUPPORT OUTER PLANET MISSIONS

by

Henry F. Fliegel
and
C. C. Chao

Jet Propulsion Laboratory
California Institute of Technology

ABSTRACT

Navigation of Mariner spacecraft to Jupiter and beyond will require greater accuracy of positional determination than heretofore obtained if the full experimental capabilities of this type of spacecraft are to be utilized. Advanced navigational techniques which will be available by 1977 include Very Long Baseline Interferometry (VLBI), three-way Doppler tracking (sometimes called quasi-VLBI), and two-way Doppler tracking. It is shown that VLBI and quasi-VLBI methods depend on the same basic concept, and that they impose nearly the same requirements on the stability of frequency standards at the tracking stations. It is also shown how a realistic modelling of spacecraft navigational errors prevents overspecifying the requirements to frequency stability.

****

Several papers delivered at this conference deal with Very Long Baseline Interferometry (VLBI), by which the difference between the times of arrival of a signal at two widely separated stations from a distant radio source is determined by cross-correlation of data tapes. The Jet Propulsion Laboratory is supplementing its VLBI program with a simpler technique, similar in principle but requiring far less data processing, which is informally called Quasi-VLBI (QVLBI). Although developed primarily to solve problems in spacecraft navigation, QVLBI can be used to compare the frequencies and time rates of change of frequency of widely separated oscillators.

By the methods which are now conventional at JPL, only two kinds of data are available for the radio navigation from the Earth of a distant spacecraft. The range may be determined by measuring the time

required for a radio signal to travel to the spacecraft and back; and the range rate can be obtained from the doppler shift of the returned signal. Of course, these two data types determine only one mathematical function, since the second is merely the time derivative of the first. The fundamental problem of spacecraft navigation is that, of the three coordinates which an astronomer would use to locate an object in space -- radial distance, right ascension, and declination -- only the first is measurable using a single antenna, and the angular position must be deduced. At best, this deduction is difficult.

Several kinds of information are contained in the measurements of range rate, and only by combining them can the deduction of spacecraft position and velocity be made reliably. In Figure 1, bottom, the sinusoidal curve shows the effect of the rotation of the Earth on the frequency of the returned signal by the doppler effect. Where the spacecraft is below the horizon of the tracking station (that is, from spacecraft set to spacecraft rise), the plotted curve is dashed; the solid portion of the curve represents observable data. Since the phase of the curve depends on spacecraft right ascension and the Earth's rotational angle (UT1), the right ascension can be determined if UT1 is known; similarly, spacecraft declination can be determined from the amplitude of the curve. The uncertainty in our ability to target the spacecraft is represented by an elliptical area in a plane constructed perpendicular to the vector of spacecraft motion, within which the spacecraft is located to a certain confidence level, as illustrated at the top of Figure 1. As the spacecraft approaches the target planet, the gravitational pull causes a rapid change in the measured range rate (bottom of Figure 1). Not shown in Figure 1 is the small but measurable change in the gravitational acceleration of the spacecraft toward the Sun, which is a function of position of the spacecraft in its orbit, and which can therefore be used to infer that position. All these kinds of information have been used via the Double-Precision Orbit Determination Program (DPODP) at JPL to ascertain and then to correct the trajectory parameters of the Mariner and Pioneer spacecraft during the successful missions of the past twelve years. Until now, range and range rate information obtained by one tracking station at any given time (single station tracking) has been adequate to meet all mission requirements.

However, as requirements become more stringent, the sources of error in single station tracking become quite serious. Consider the case illustrated in Figure 2, in which a spacecraft is traversing a long path (say to Jupiter), and in which data is being accumulated for many days to render the gravitational bending of the vehicle toward the Sun most noticeable (the long arc method). This acceleration toward the Sun varies from only 6mm/sec^2 to 0.2 mm/sec^2 over the entire distance from Earth to Jupiter, and, over the last 100 million kilometers of distance travelled, changes by only 33%. Large uncertainties can be produced by small effects -- by non-gravitational forces such as gas leaks, by changes made to the spacecraft trajectory (maneuvers) if they cannot be

perfectly modelled, and by unforeseen events (meteor impact, sudden venting of gas, and the like). The effect of the rotation of the Earth in controlling the spacecraft position determination through the diurnal doppler signature can be corrupted by the ionosphere and by the uncertainty in station longitude. And the effect of the gravitational pull of the target planet usually appears too late to be helpful for use in guidance. The basic difficulty is that spacecraft position is very difficult to determine by range (or range rate) information from a single tracking station.

Figure 3 illustrates what can be measured when two antennas track the spacecraft simultaneously, and the logic is very similar to that of VLBI. In going from single station to two station tracking, we have passed from so-called two-way ranging to three-way ranging. Single station tracking is called two-way ranging because there is an uplink (station transmitting to spacecraft transponder) plus a downlink (transponder replying to station). If a second station listens, but does not transmit, there is a third link (called the "three-way downlink"). The physically significant quantity in the situation is the difference, τ, in the time of arrival of spacecraft signal between the two stations; and if $\vec{B}$ is the baseline vector between the two stations, $\vec{s}_1$ is the unit vector indicating spacecraft direction, and c is the speed of light, then

$$\tau = \frac{\vec{B} \cdot \vec{s}_1}{c} \quad , \tag{1}$$

which is the fundamental equation of VLIB. If the fractional frequencies of received signal at the two stations are differenced, this difference (called "two-way minus three-way doppler") is the dimensionless quantity $\dot{\tau}$, the time rate of change of τ. These new data types, τ or $\dot{\tau}$, as reduced from two-way and three-way range and doppler data, are called Quasi-VLBI (QVLBI).

The advantage of QVLBI for spacecraft navigation over single-station tracking is that the angular position of the spacecraft can be directly measured, and not merely inferred by the orbit determination program. But QVLBI also offers the possibility of measuring the frequency offset between the widely separated station oscillators. If these oscillators were perfectly synchronized, then one would measure

$$\left(\frac{\Delta f}{f}\right)_{\text{observed}} = \dot{\tau} = A \cos \omega t \text{ (from the Earth's rotation)} + \text{atmospheric effects} + \text{equipment delay effects} \tag{2}$$

The atmospheric effects are caused especially by the difference in charged particle content in the ionosphere over the two stations, and by the difference in water vapor content in the troposphere, which is

difficult to model. The equipment delays (for example, cable delays) will produce no effect if they are constant, but any variation (for example, temperature effects at sunrise) will map directly into the observed frequency offset. If the station frequency standards operate at different frequencies, then the last equation becomes

$$(3) \quad \left(\frac{\Delta f}{f}\right)_{\text{observed}} = A \cos \omega t + \left(\frac{\Delta f}{f}\right)_{\text{standard}} + \ldots$$

where (. . .) represents the atmospheric and equipment effects. Notice that, given sufficient data (i.e., a sufficient number of observational equations of the form of Equation (3) one can solve for A and $\Delta f_{\text{standard}}$ separately; furthermore, by expanding $\Delta f_{\text{standard}}$ in a Taylor series, one could in principle solve for any number of coefficients in the polynomial expansion of Δf. In practice, the atmospheric sources of error make it impractical to solve for terms higher than frequency and frequency rate; Equation (3) becomes

$$(4) \quad \left(\frac{\Delta f}{f}\right)_{\text{observed}} = A \cos \omega t + \left(\frac{\Delta f}{f}\right)_{\text{standard}} + t \cdot \left(\frac{\dot{\Delta f}}{f}\right) + \ldots$$

These simplified QVLBI equations illustrate the basic principles. In practice, solutions from real data have been made using the Double Precision Orbit Determination Program (DPODP), which estimates frequency standard and spacecraft trajectory parameters simultaneously.

In 1971, the Mariner 9 spacecraft was simultaneously tracked by the Echo Deep Space Station (DSS 12) at Goldstone, California, and DSS 41 at Woomera, Australia, (no longer operational) during the month and a half prior to Mars encounter. It was the first time that the QVLBI technique was demonstrated with real tracking data. The results, though promising, were not as conclusive as might be hoped due to the limited amount of data and inadequate knowledge about the behavior of the frequency and time system employed. Later in 1973, a series of short baseline ($\approx$15 km) two station doppler demonstrations with the Pioneer 10/11 spacecrafts was initiated to understand better the nature of variations of the frequency and timing system. Results indicate that the frequency offsets between stations vary slowly and linearly with a long-term ($\approx 10^6$ sec) stability on the order of 2 parts in 10^{12} ($\Delta f/f$). A successful QVBLI demonstration with real tracking data was made in December 1973 during the Jupiter Encounter of Pioneer 10 spacecraft. On the basis of this experience, a real-time demonstration of the QVLBI technique was planned and carried out during the Mariner 10 mission to Venus and Mercury (MVM).

MVM was the first interplanetary mission using one spacecraft to fly by two planets (Venus and Mercury) with the assistance of the gravitational attraction of one of the two planets. The official mission was successfully completed with the Mercury encounter of 29 March 1974, and was extended to have a second flyby of the planet Mercury on 21 September. The trajectory of Mariner 10, which is shown in Figure 4, consisted of many segments, each segment terminated by either planetary encounter or a trajectory correction maneuver (TCM). Therefore our demonstration was divided into five portions according to the following time spans:

1. TCM-1 to TCM-2 (from November 13, 1973 to January 21, 1974)
   Orbital determination solutions from this segment were used for TCM-2 in order to bring the space probe to the desired aiming point at Venus encounter.

2. TCM-2 to Venus encounter (from January 21 to February 5, 1974)
   This segment covered the closest approach to Venus, so that the position of the probe was accurately determined and provided a reference to compare solutions from the differenced doppler technique with conventional data.

3. Venus encounter to TCM-3 (from February 5 to March 16)
   This segment was to determine the trajectory to provide the parameters for TCM-3.

4. TCM-3 to Mercury encounter (from March 16 to March 29)
   This provided another opportunity to demonstrate the short arc ($10 \sim 12$ days) orbital determination capabilities using differenced doppler data.

5. TCM-4 to TCM-5 (from May 10 to June 24)
   This segment was in the extended mission phase (after Mercury flyby) and covered the superior conjunction, which offered an excellent opportunity to demonstrate how well the effects of noise from the solar corona could be removed.

The demonstration was successful in providing estimates of spacecraft velocity and position free of corrupting influences. It is especially interesting to consider the estimates which the data provided of the offsets between frequency standards.

Figure 5 illustrates two different types of estimate of frequency offsets between oscillators at the participating stations. All results

are with respect to the DSS 14 (Mars) antenna frequency standard at Goldstone, California; other participating stations were DSS 12 (Echo) 16 km south of Mars antenna at Goldstone; DSS 42 and 43 in Australia, which shared a single frequency standard; and DSS 62 and 63 in Spain, each with its own standard. All stations used Hewlett-Packard 5065A rubidium standards for MVM navigation.

The first type of estimate is shown by the heavy black diamonds in Figure 5, each of which gives the solution from a single day's tracking data for Δf in millihertz between Mars and Echo oscillators (12 minus 14) at Goldstone. Since the tracking frequency is S-band (2.3 gigahertz), 7 millihertz corresponds to $\Delta f/f = 3$ parts to 10^{12}, the size of largest residual from the mean which occurred. Since these stations are so close (16 km.), both looked through virtually the same atmosphere, and the relative longitudes are known to within 6 cm., so that the results are nearly the best attainable by the present technique. We believe that these results display the real offsets between the station oscillators, though the tendency of the data to return to the mean value from the highest residuals, rather than to execute a random walk, is perhaps suspicious. Every user of VLBI or related techniques for clock or frequency standard comparison must observe that what is measured is the offset of an entire system -- antenna, cables, circuitry, and oscillator, under the local atmosphere -- rather than of the oscillator alone. In this case, we have no reason to suppose that effects other than frequency standard offset and drift are present, but the possibility cannot be ruled out completely.

The second type of estimate is displayed by the open circles, squares, and triangles in Figure 5. For each station, and for each of the time periods defined above, all tracking data were combined by the Orbit Determination Program, and estimates were formed of (1) frequency offset (2) standard deviation of the estimated frequency offset (3) rate of change of offset, when the estimate for rate was believed to be statistically significant. The estimates thus formed for DSS 12 and 14 agree fairly well with the black diamonds. The estimates for rate correspond fairly well with the differences between offsets estimated on different dates. The error bars were estimated by the Orbit Determination Program using a priori values of station longitude uncertainty of 5 meters; this estimate probably errs on the pessimistic side for stations of the Deep Space Net (DSN), but gives a fair idea of the uncertainties to be expected when conditions are not optimal. The extremely large errors bars on the right represent the data when the spacecraft was near the Sun as seen from Earth.

These data indicate that frequency offsets can be measured to a precision of 1 part in 10^{12} under fair conditions (error bars, Figure 5) to about 1 part in 10^{13} under the best conditions (scatter of black diamonds.)

The experiments reported here have been very useful in studies of what precision of frequency standard is needed for navigation in the DSN. They indicate that the behavior of the frequency standards can be modelled using solve-for parameters, along with spacecraft state, and so prevent us from overspecifying DSN standards. It has been shown at JPL that the existing rubidium standards were adequate to the needs of the MVM mission, but that requirements for outer planet missions will require the use of H-masers.

ORBIT DETERMINATION INFORMATION FROM PERTURBATION OF SPACECRAFT BY PLANET

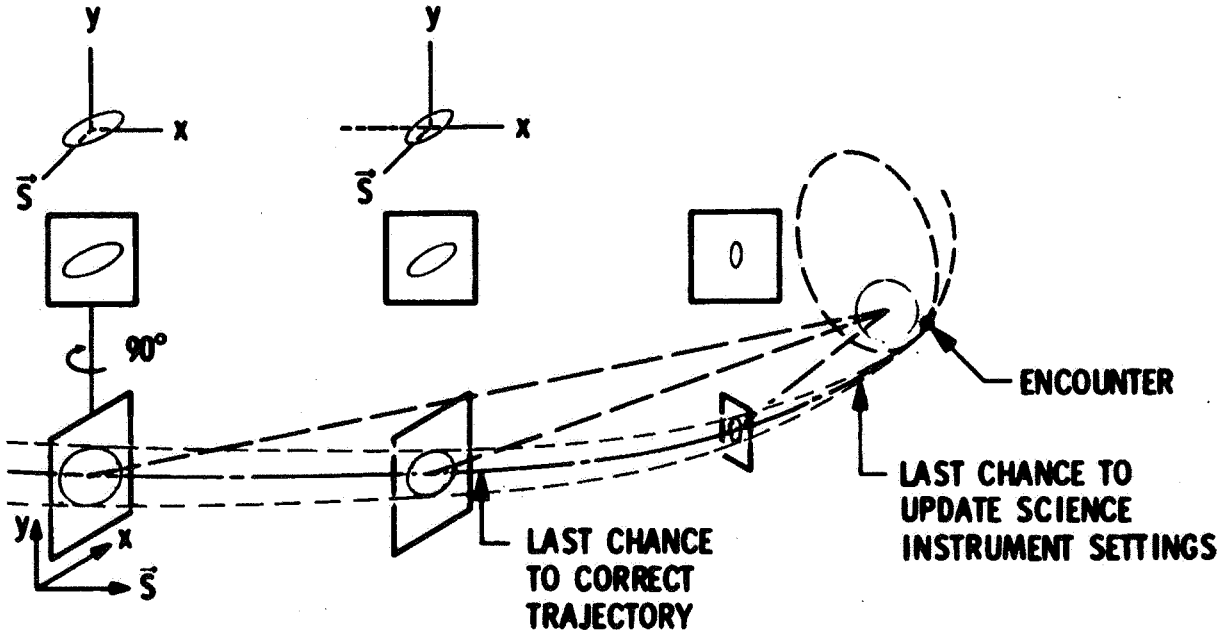

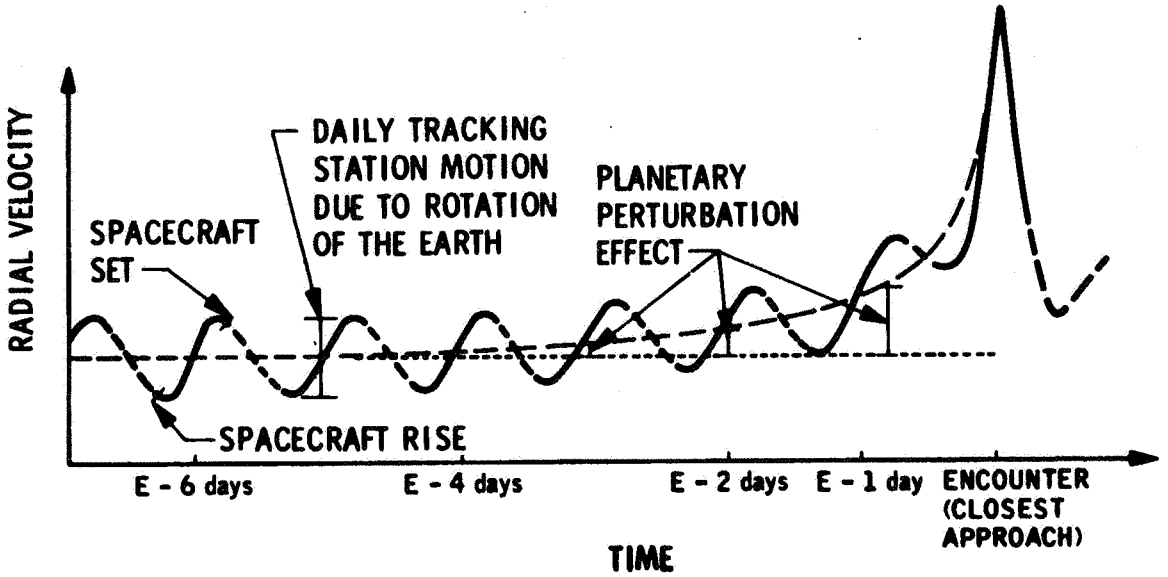

FIGURE 1

LONG ARC METHOD OF SPACECRAFT NAVIGATION

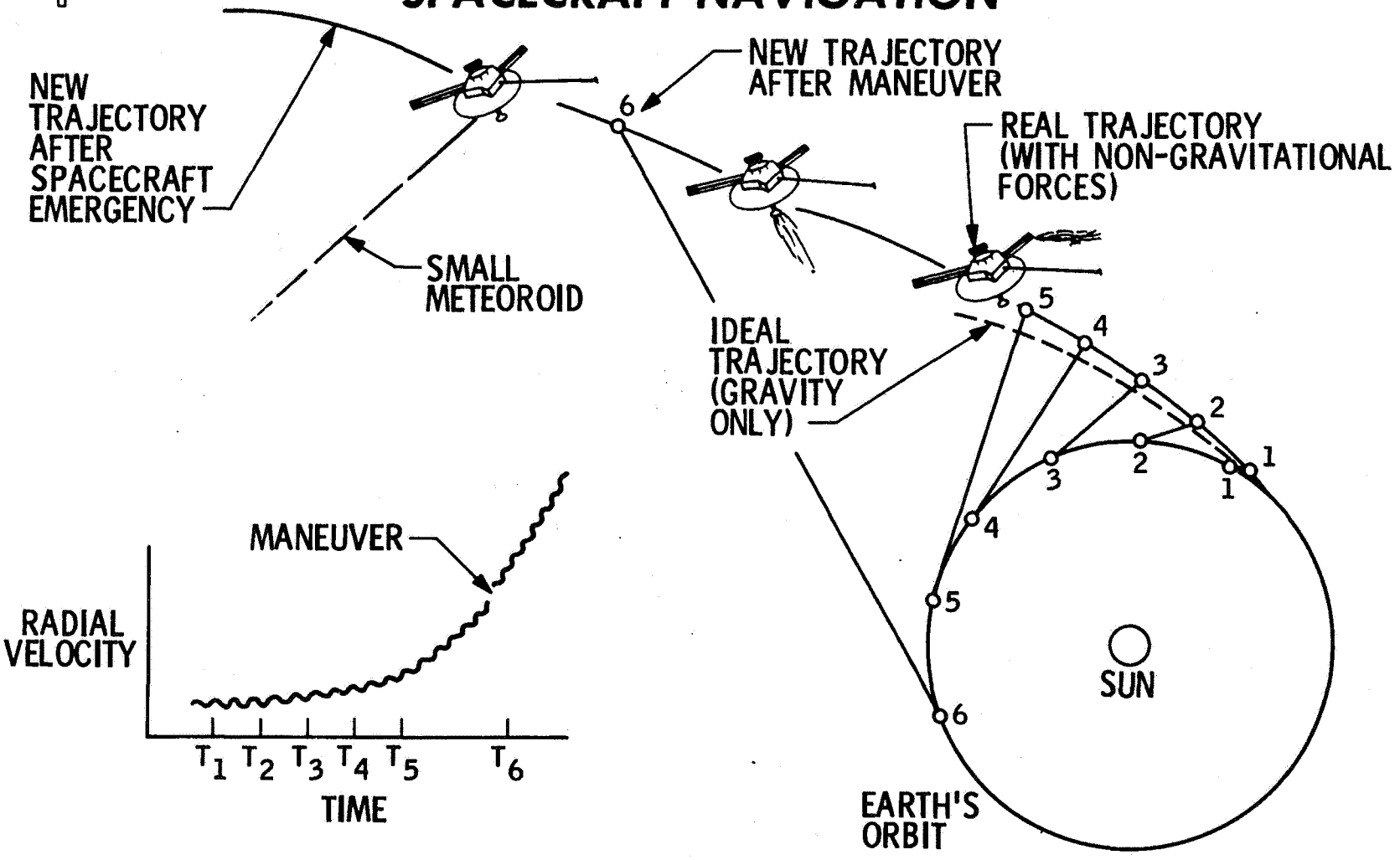

FIGURE 2

GEOMETRY OF QUASI-VLBI
(TWO AND THREE WAY TRACKING)

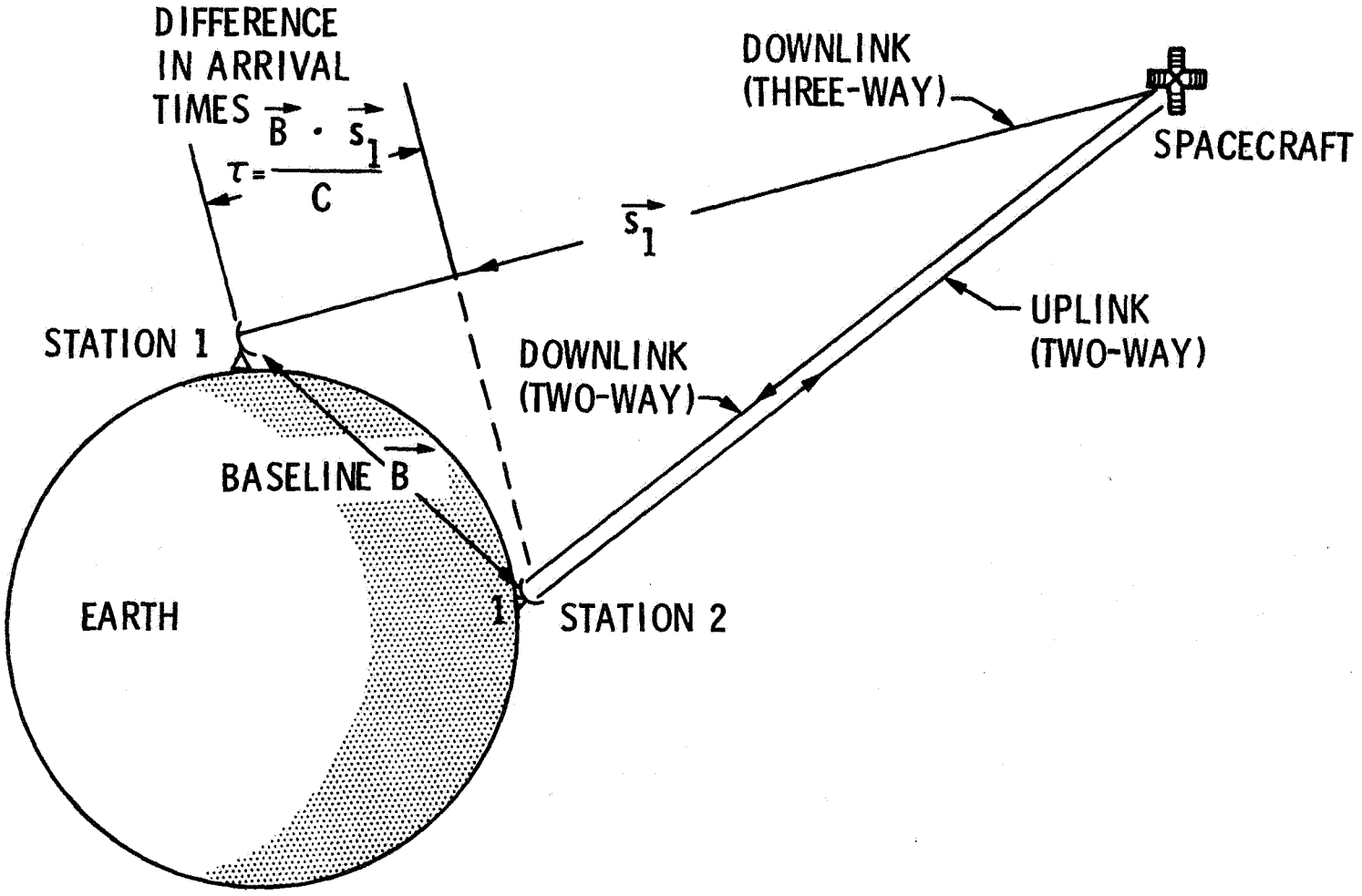

FIGURE 3

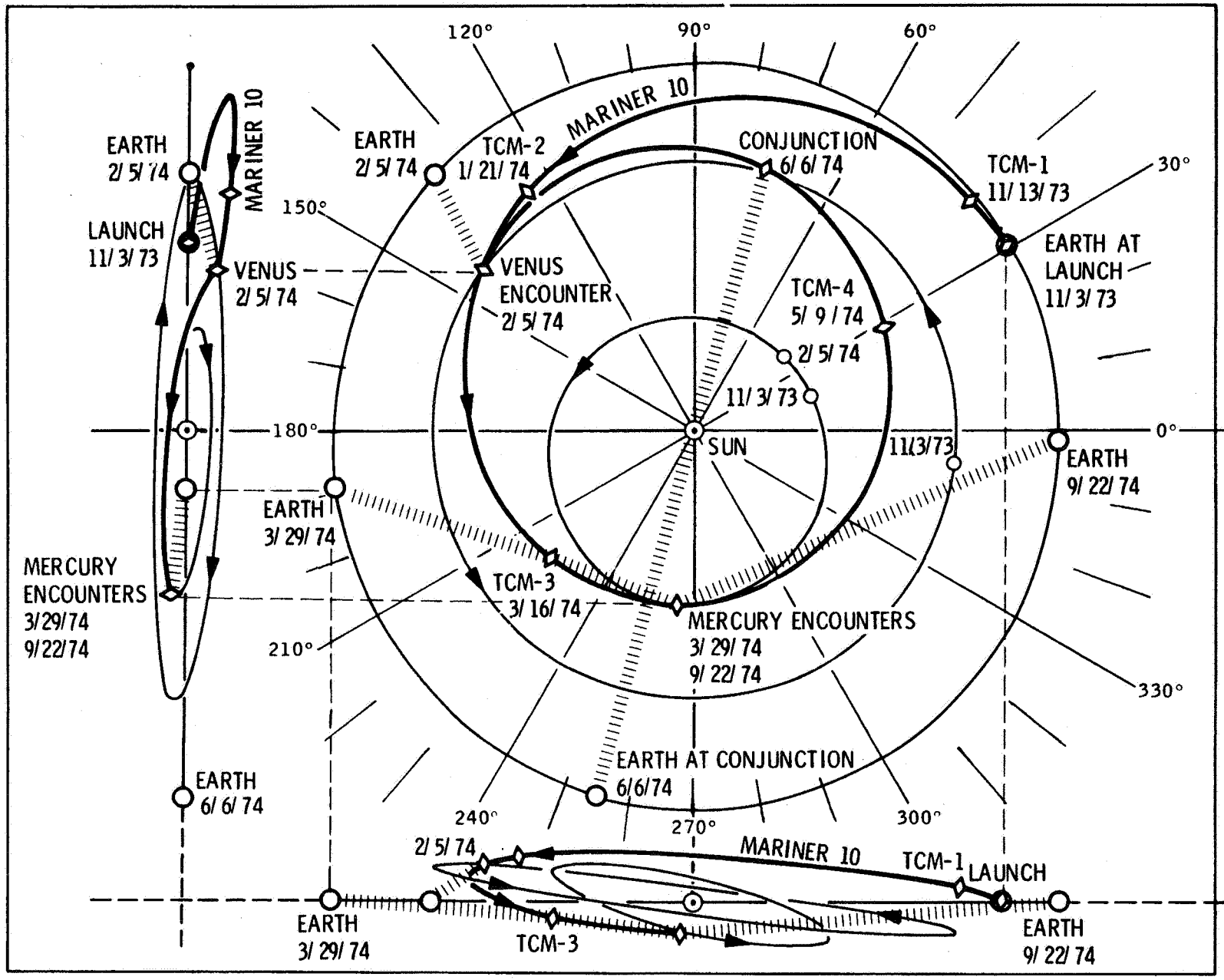
120°
90°
60°
MARINER 10
EARTH
2/5/74
MARINER 10
EARTH
2/5/74
TCM-2
1/21/74
CONJUNCTION
6/6/74
TCM-1
11/13/73
30°
150°
LAUNCH
11/3/73
VENUS
2/5/74
VENUS
ENCOUNTER
2/5/74
TCM-4
5/9/74
2/5/74
EARTH AT
LAUNCH
11/3/73
11/3/73
180°
SUN
11(3/73
0°
EARTH
9/22/74
EARTH
3/29/74
MERCURY
ENCOUNTERS
3/29/74
9/22/74
TCM-3
3/16/74
MERCURY ENCOUNTERS
3/29/74
9/22/74
210°
330°
EARTH AT CONJUNCTION
6/6/74
EARTH
6/6/74
240°
270°
300°
2/5/74
MARINER 10
TCM-1
LAUNCH
EARTH
3/29/74
TCM-3
EARTH
9/22/74

FIGURE 4

VALUES OF ESTIMATED FREQUENCY OFFSET RELATIVE TO DSS14

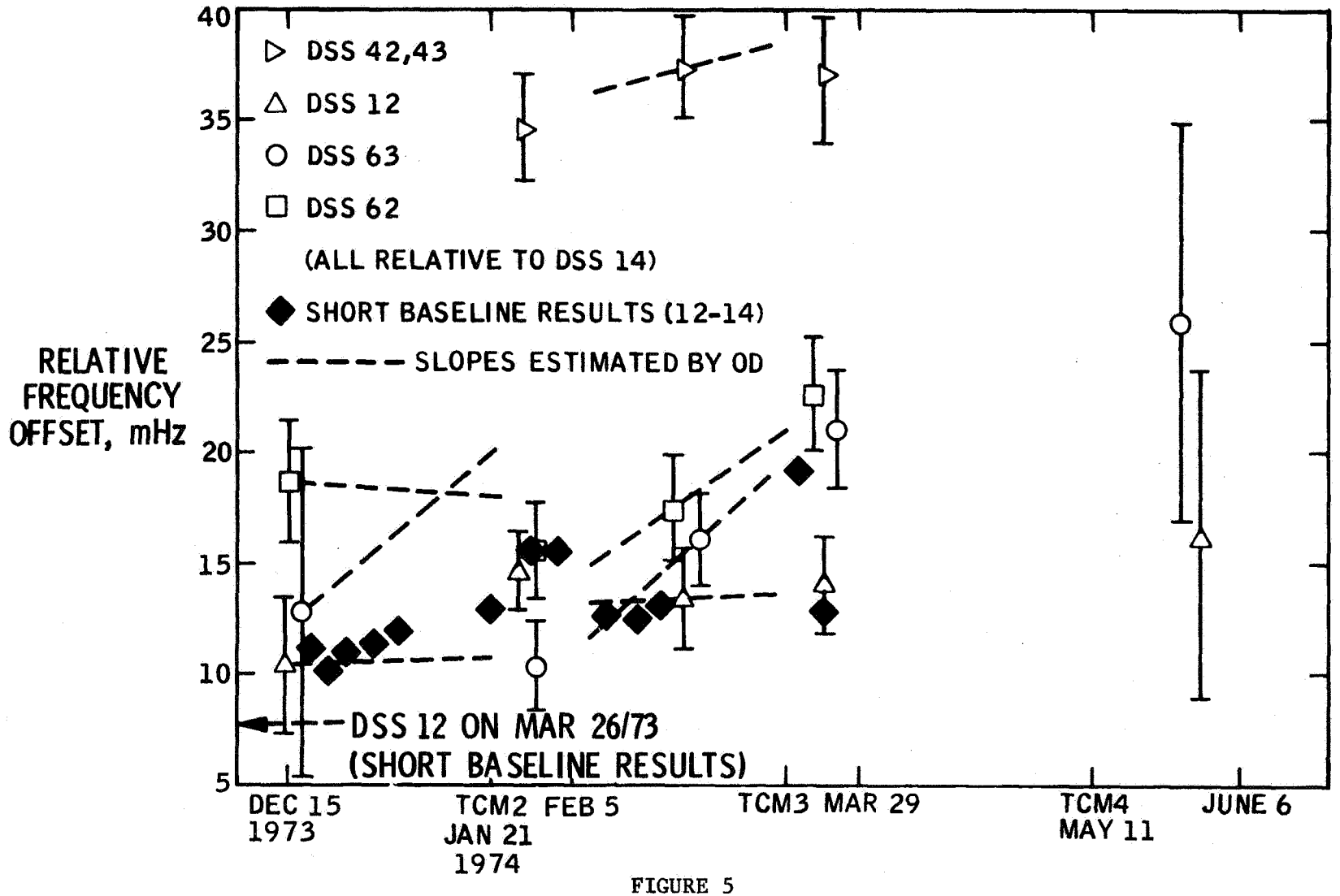

FIGURE 5